Electronic Supplementary Information

Nickel macrocycles with complex hydrides – new avenues for hydrogen storage research

Andrew James Churchard,* Michał Cyranski, Łukasz Dobrzycki, Armand Budzianowski, and Wojciech Grochala

S1. Additional Experimental Details

Preparation of cyclam precursors from NiL_x, $L_x = SO_4$, $(BF_4)_2$, $(ClO_4)_2$

$NiSO_4$•$6H_2O$ (Aldrich), $Ni(BF_4)_2$•$6H_2O$ (ABCR) or $Ni(ClO_4)_2$•$6H_2O$ (ABCR) was dissolved in anhydrous methanol (Aldrich) with dimethoxypropane (ABCR) used as dehydrating agent. A slight molar excess (5–10%) of cyclam (ABCR) was dissolved separately in anhydrous methanol with dimethoxypropane, and the two solutions mixed. A coloured precipitate quickly formed ([Ni(cyclam)(SO_4)] – pink, [Ni(cyclam)(ClO_4)$_2$] – yellow–orange, Ni(cyclam)(BF_4)$_2$ – orange) which was separated, washed repeatedly with anhydrous methanol and left to dry in the glovebox at room temperature.

Alternative synthesis of trans-Ni(cyclam)(BH_4)$_2$: reactions of [Ni(cyclam)L_x] ($L_x = SO_4$, $(BF_4)_2$, $(ClO_4)_2$) with $NaBH_4$, $NaBD_4$ and $(C_4H_9)_4NBH_4$

Reactions were carried out either with solutions of reactants or with pre–mixed solid reactants ground in a mortar and pestle from which a slurry was formed. Solutions of approximately 0.1 M $NaBH_4$ and $NaBD_4$ in anhydrous acetonitrile (Aldrich, further dried over CaH_2), and approximately 0.02 M ligated [Ni(cyclam)L_x] complexes were prepared. Reactions were carried out with both excess $NaBH_4$/$NaBD_4$ and stoichiometric quantities (i.e. 2:1 $NaBH_4$: [Ni(cyclam)L_x]). The resulting solid (trans–Ni(cyclam)(BH_4)$_2$) was separated and washed with dry THF and left in the glovebox to dry.

High–energy disc milling and mechanochemical doping

All milling was carried out in a vibrational disc mill (Testchem) using tungsten carbide mill pieces and a milling time of 3 minutes.

We attempted to synthesise Ni(cyclam)(BH_4)$_2$ via mechano–chemical metathetical (ligand exchange) by milling Ni(cyclam)(SO_4) with $NaBH_4$ as this could bring benefits in terms of cost and environmental considerations (no use of solvent). However, simply milling the two compounds did not produce a chemical reaction; the powder x–ray diffraction pattern showed a superposition of the two original phases (see below).

Crystallisation and x–ray structural measurements

Single crystals of trans–Ni(cyclam)(BH_4)$_2$ (green rods) were obtained directly from an alternative synthetic pathay in acetonitrile followed by quick (1 hr) spontaneous crystalllisation. Single crystals of cis–Ni(cyclam)(BH_4)$_2$ were grown from a very dilute solution of the compound in dry THF by slow evaporation over a period of approximately 2 weeks, inside the glovebox.

Measurements of both crystals were performed on a KM4CCD □-axis diffractometer with graphite-monochromated MoK□ radiation at T=100 K. The crystals were positioned 62 mm from the CCD camera. The data were corrected for Lorentz and polarization effects. Empirical corrections for absorption were applied[1]. Data reduction and analysis were carried out with the Oxford Diffraction programs[2].

Both structures were solved by direct methods[3] and refined using WinGX[4] and SHELXL[5]. The refinements were based on F^2. Scattering factors were taken from Tables 6.1.1.4 and 4.2.4.2 in Ref. 6.

In the structure of trans–Ni(cyclam)(BH_4)$_2$ coordinates of all atoms were refined. The temperature factors of all heavy atoms were refined anisotropically. The temperature factors of hydrogen atoms were not refined and were set to be equal to either 1.2 or 1.8 times larger than U_{eq} of the corresponding heavy atom. In the case of the heavily disordered cis–Ni(cyclam)(BH_4)$_2$, the geometrical restraints for C–C and C–N distances were applied with the goal set to be equal to 1.52 Å and 1.48 Å respectively (instruction with esd = 0.02). All hydrogen atoms of the macrocycle were located geometrically and their positions were not refined. Hydrogen atoms of both BH_4^- anions were constrained to form tetrahedra with B–H distances fixed in range 1.06–1.19Å. Only the rotation of BH_4^- moieties was free to refine leading to a reasonable orientation. The temperature factors of all heavy atoms were refined anisotropically. The temperature factors of hydrogen atoms were not refined and were set to be equal to either 1.2 or 1.5 times larger than Ueq of the corresponding heavy atom.

---

[1] CrysAlis RED, Oxford Diffraction Ltd., Version 1.171.33. Empirical absorption correction using spherical harmonics, implemented in SCALE3 ABSPACK scaling algorithm.

[2] CrysAlis CCD, Oxford Diffraction Ltd., Version 1.171.33, CrysAlis RED, Oxford Diffraction Ltd., Version 1.171.33.

[3] G. M. Sheldrick, Acta Crystallogr. 1990, **A46**, 467-473.

[4] L. J. Farrugia, J. Appl. Cryst., 1999, **32**, 837-838.

[5] G. M. Sheldrick, SHELXL93. Program for the Refinement of Crystal Structures., Univ. of Göttingen, Germany.

[6] International Tables for Crystallography, Ed. A. J. C. Wilson, Kluwer: Dordrecht, 1992, Vol. C.

FTIR spectroscopy

IR spectra were recorded on a Bruker vertex 80 FTIR spectrometer in KBr pellets in an evacuated chamber. The pellets were formed inside the glovebox thus avoiding prolonged exposure to atmosphere.

TGA/DSC with evolved gas analysis (EGA) measurements

Typically, 7 mg of analyte was loaded into an alumina crucible and measured using a Netzsch STA 409 PG TGA/DSC coupled to a Bruker Vertex 80v FTIR spectrometer and Netzsch QMS 403 C mass spectrometer via transfer lines and adapter heads heated to 200°C. Typical experiments were over the temperature range 25–300°C using a 1, 2 or 3 K min^{-1} scanning rate. 1 K min^{-1} was used to allow clearer separation of the decomposition steps and 2 or 3 K min^{-1} as a compromise between separating the steps and achieving a reasonable concentration of evolved gas in the flows to the EGA instruments.

Ice forming on the FTIR detector occasionally causes a wide band to form between 3060–3620 cm^{-1}. This is subtracted from the spectra using a background spectrum for this ice band.

EGA MS ion–currents for each m/z value were normalised such that the minimum ion current for that m/z value over time is set to 1. This means that the values reported in this paper are a multiple of the minimum signal for that m/z value over the whole experiment. The rationale for this approach is that, aside from situations where scavenging occurs, the lowest ion–current will approximate to the background value. Signals that can be seen to be clearly different from background using this method are lost when comparing relative intensity for each scan (i.e., across the whole m/z spectrum at one point in time) due to the huge differences in background ion–current for different m/z. This method allowed us to track changes in signals more easily, but with the effect that isothermal values for different m/z values should not necessarily be considered relative to one another as one would in a typical mass spectrum.

The synchronisation of the EGA–MS and EGA–FTIR signals was calibrated using CuSO4 x 5 H2O. Both were found to respond within 15 seconds, which for the 3 K min^{-1} measurements corresponds to a discrepancy of < 0.75 K between TGA and evolved gas detection.

Density Functional Theory (DFT) calculations

The DFT optimizations at the B3LYP/6-311++G** level were performed for both neutral trans–Ni(cyclam)$(BH_4)_2$ and charged cis–Ni(cyclam)$(BH_4)^+$ moiety, for two distinct spin states (low-spin singlet, high-spin triplet). See below for details.

S2. Results of attempted mechanochemical synthesis of Ni(cyclam)$(BH_4)_2$ by milling Ni(cyclam)(SO_4) with $NaBH_4$

We attempted to synthesise Ni(cyclam)$(BH_4)_2$ via mechano–chemical metathetical (ligand exchange) by milling Ni(cyclam)(SO_4) with $NaBH_4$ as this could bring benefits in terms of cost and environmental considerations (no use of solvent). However, milling the two compounds for 3 minutes did not produce a chemical reaction; the powder x–ray diffraction pattern showed a superposition of the two original phases (see figure ESI_1).

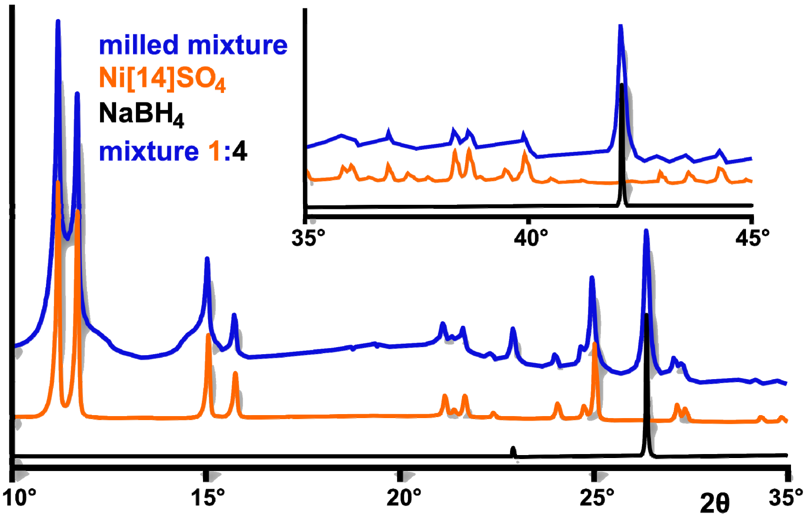

Fig ESI_1: Powder x-ray diffraction patterns of $NaBH_4$ (black), Ni(cyclam)SO_4 (orange), and a milled mixture of the two (blue), in a mol ratio of 1:4, Ni(cyclam)SO_4:$NaBH_4$

S3. Additional discussion of single crystal X-ray diffractions

In the crystal lattice of the trans isomer, interacting molecules form parallel rows extending in the [100] direction. The shortest intermolecular contact at 2.31 Å can be observed between an H(5) atom of the BH_4^- group and an amine H(1) atom. Thus, the orientation of BH_4^- provides formation of almost equal intra- and intermolecular dihydrogen H···H contacts but the compound can nevertheless clearly be considered a molecular crystal.

The cis isomer of Ni(cyclam)$^{2+}$ is much less commonly found in the solid state than its trans analogue, as confirmed by a CSD search. There are 107 Ni(cyclam)$^{2+}$–containing structures deposited in the CSD but only 11 of them are of the cis type.
The cis isomer displays dihydrogen bonding[7], most strongly between hydrogen atoms H2BC (of the non-coordinated BH_4^- group) and H2N, with dH–H = 2.06 Å. Two further hydrogens of this BH_4^- group interact more weakly with H4N, where dH–H = 2.15 Å and 2.19 Å. The dihydrogen bonding markedly red-shifts the bands corresponding to the NH stretching modes in the IR spectra (see Fig.3). The bidentate coordinated BH_4^- group, engaged in strong bonding to Ni, shows only weak dihydrogen bonding, with the closest contact at dH–H = 2.26 Å, between H1BD and H3N. This distance is greater than that typically found for strong dihydrogen bonding (1.7-2.2 Å [8]), but still less than that of the van der Waals radii of two H atoms (2.4 Å).

As stated in the main article, the crystal structure of the cis isomer is severely disordered, similar to its trans-perchlorate analogue[9]. The [cis-Ni(cyclam)(BH_4)]$^+$ cation is located on a mirror plane passing through Ni(1), B(1) and B(2) atoms. Because the single cis-Ni(cyclam) moiety is chiral this operation generates two overplayed species with ½ occupancy each. Such disorder is of the static type. See figure ESI_2 for an illustration of this effect.

---

[7] A. Bondi, *J. Phys. Chem.*, 1964, **68**, 441-451

[8] W. T. Klooster, T. F. Koetzle, P. E. Siegbahn, T. B. Richardson, and R. H. Crabtree, *J. Am. Chem. Soc.*, 1999, **121**, 6337-6343; R. Custelcean and J. E. Jackson, *Chem. Rev.*, 2001, **101**, 1963-1980.

[9] L. Prasad, S. C. Nyburg, and A. McAuley, *Acta Crystallogr., Sect. C: Cryst. Struct. Commun.*, 1987, **43**, 1038-1042.

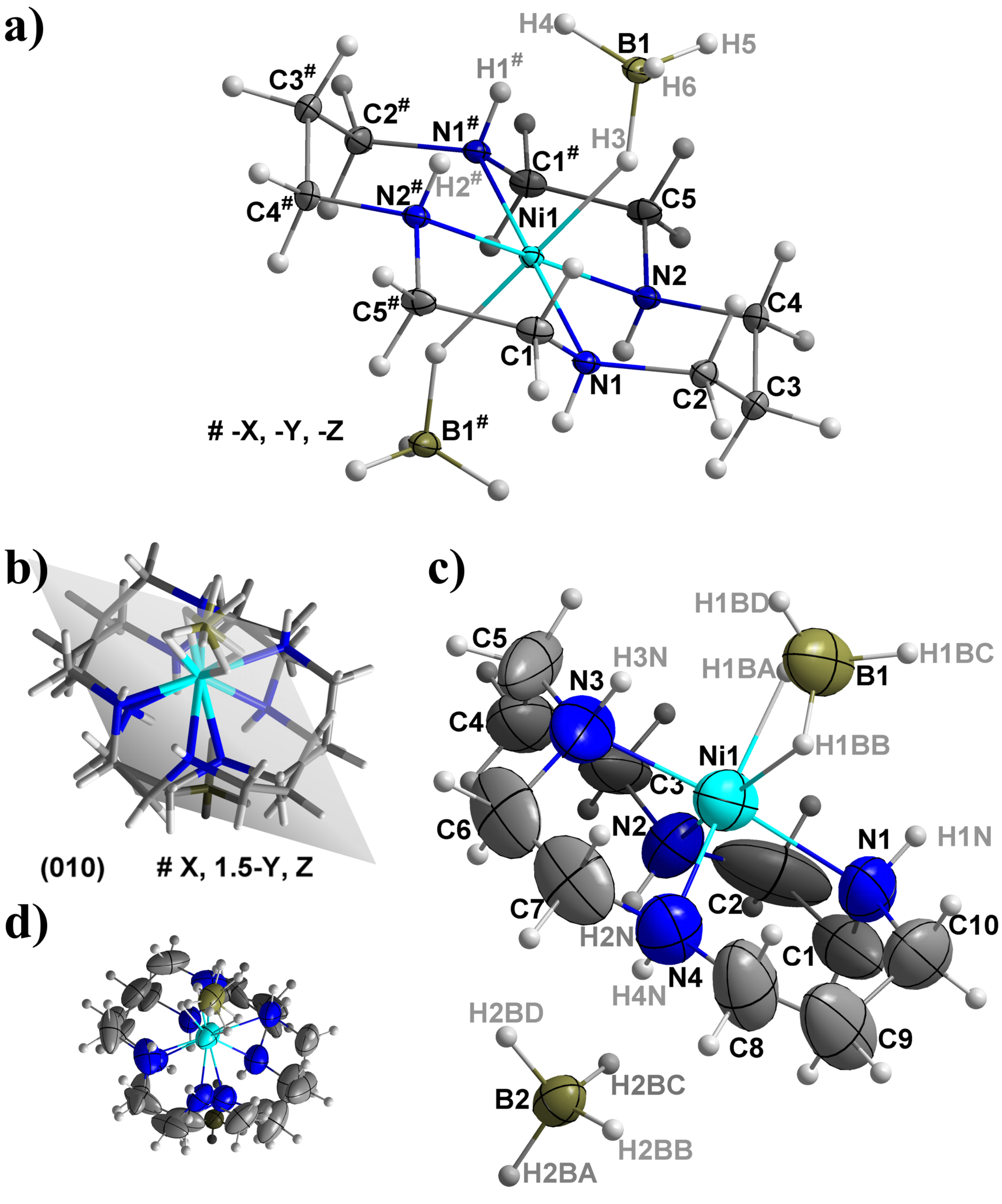

Fig ESI_2 The thermal ellipsoid representation of a) trans-Ni(cyclam)$(BH_4)_2$, b) and d) shows the cis isomer's disorder whereas c) presents only the half of the molecule. The thermal ellipsoids are at the 50% probability level.

S3. Detailed Crystal data for Ni(cyclam)$(BH_4)_2$

Table ESI_1 Crystal data and structure refinement for Ni(cyclam)$(BH_4)_2$

	Trans	**Cis**
Empirical formula	$C_{10}H_{32}B_2N_4Ni$	$C_{10}H_{32}B_2N_4Ni$
M	288.73	288.73
T/ K	100(2)	100(2)
λ/ Å	0.71073	0.71073
Crystal system, space group	Monoclinic $P2_1/c$ (No 14)	Orthorhombic $Pnma$ (No 62)
Unit cell dimensions/ Å^3, º	a=7.1397(5) b=12.8109(7) c=8.7041(5) β=109.948(6)	a=14.4512(7) b=9.4625(6) c=11.7824(7)
V/ Å^3	748.36(8)	1611.18(16)
Z, D_x/ g·cm^{-3}	2, 1.281	4, 1.190
μ/ mm^{-1}	1.282	1.191
$F_{(000)}$	316	632
Crystal size/ mm	0.20×0.14×0.11	0.22×0.15×0.10
θ_{min}/ º , θ_{max}/ º	2.95, 28.58	2.76, 25.49
Reflections collected / unique	6841 / 1820 R_{int}=0.0130	12412 / 1598 R_{int}=0.0496
Completeness	98.3 %	99.9 %
Absorption corr.	Semi-empirical	Semi-empirical
T_{max}, T_{min}	0.87, 0.79	0.890, 0.801
Refinement method	Full-matrix LSQ on F^2	Full-matrix LSQ on F^2
Data / restraints / parameters	1820 / 0 / 100	1598 / 14 / 148
GooF F^2	1.068	0.818
R [I>2σ(I)]	$R1$=0.0190, $wR2$=0.0501	$R1$=0.0363, $wR2$=0.0873
R (all data)	$R1$=0.0251, $wR2$=0.0511	$R1$=0.0943, $wR2$=0.0951
Extinct. coeff.	0.0150(14)	-
Largest diff. peak and hole/ e·Å^{-3}	0.354, -0.277	0.326, -0.179

S4. Description and analysis of FTIR data and Raman data

Raman spectra were obtained using a dispersive T64000 Raman spectrometer (Jobin Yvonne–Spex, 647.1 nm holographic grating) equipped with an optical microscope BX40 (Olympus, 50 mm lense)

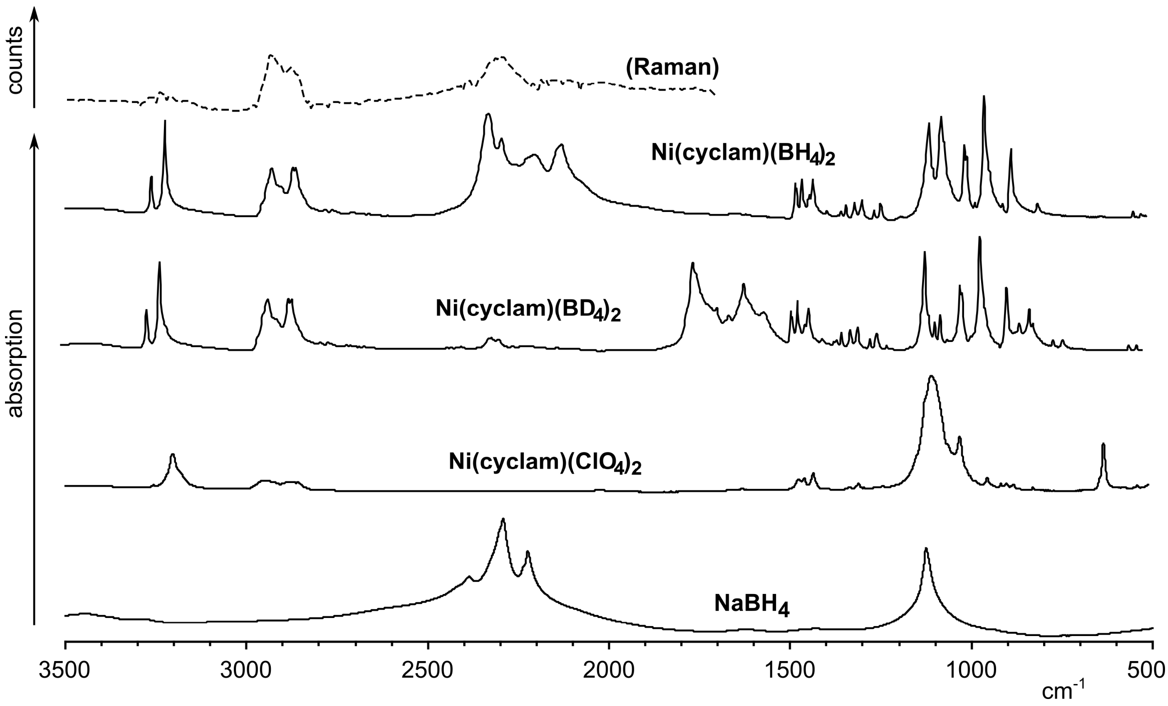

Figure ESI_3: IR spectra of (from top) trans–Ni(cyclam)$(BH_4)_2$ (plus Raman spectrum in dashed line), trans–Ni(cyclam)$(BD_4)_2$, Ni(cyclam)$(ClO_4)_2$ and $NaBH_4$

The absorption peaks in the IR spectrum assignable to the cyclam ring are in the ranges 1410–1490 and 2830–2970 cm^{-1}, and peaks arising from BH_4 stretching in the 2000–2400 cm^{-1} region. trans-Ni(cyclam)$(BD_4)_2$ (Figure ESI_3) shows the absorption from B–D stretches at 1500–1800 cm^{-1}. The vibrations of Ni(cyclam)$(BH_4)_2$ and its deuterated analogue are of lower energy than the corresponding stretches of $NaBH_4$/$NaBD_4$, indicating weaker B–H bonding. In particular, in the former species, the shoulder at 2065 cm^{-1} is assigned to the B–H stretch of the bridging H(3) (also bound to Ni) owing to the weakness arising from donation of electron density to the Ni centre. The peaks at 1070, 1060 cm^{-1} and 813, 803 cm^{-1} in the BH/BD spectra respectively, have been assigned to boron hydrogen bending modes by noting the difference between the BH and BD spectra. The Raman spectrum for trans–Ni(cyclam)$(BH_4)_2$ is also shown for the region 1700–3500 cm^{-1}.

S5. Further analysis of TGA/DSC including evolved gas analysis data

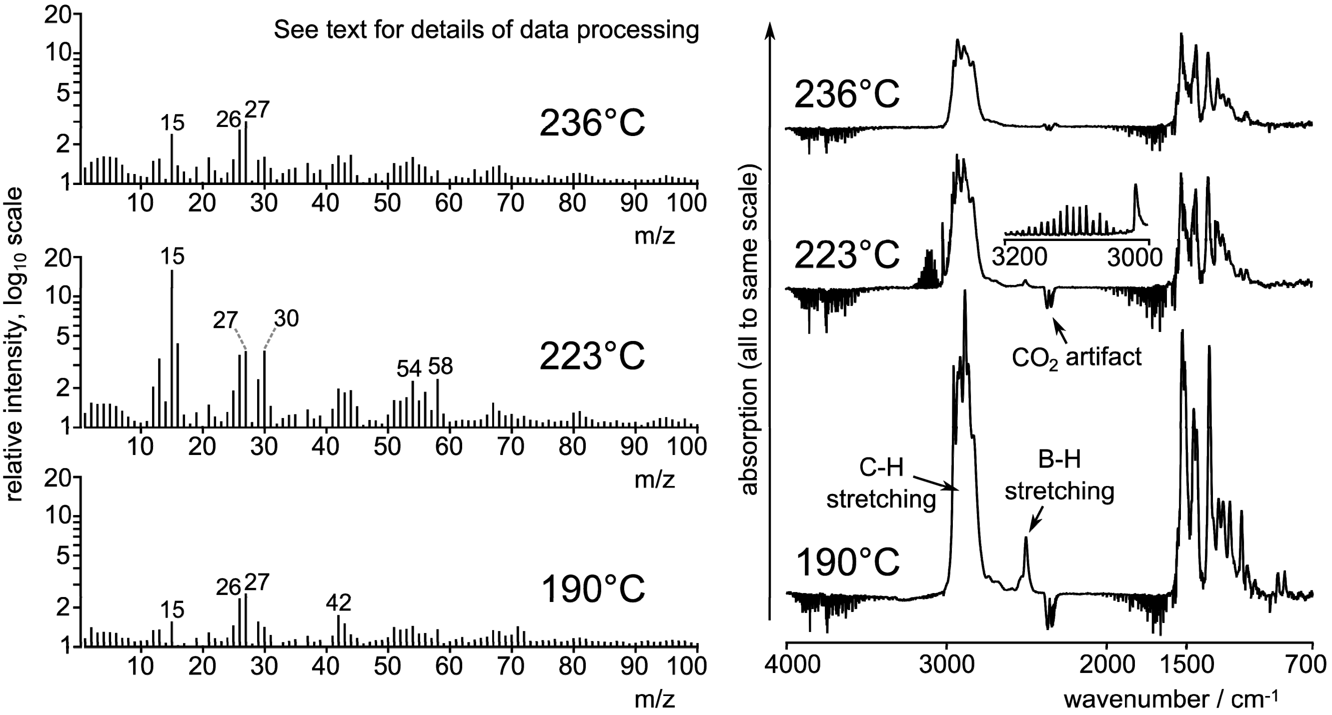

Fig. ESI_4 Evolved gas analysis of trans–Ni(cyclam)(BH$_4$)$_2$, mass spectrometry (left), FTIR (right). Temperatures correlate with the curves in figure 4, main article. See section below for details of data processing.

The thermal decomposition of trans–Ni(cyclam)(BH$_4$)$_2$ up to 300°C (see figure 4 in main paper) can be divided into two sections, distinguished from each other by two features. The first feature is the evolution of B–H containing species, evidenced by B–H stretches (2460–2560 cm^{-1}) in the EGA–FTIR (see figure ESI_4) and only occurring in the first section. The second feature is the two endothermic events occurring between 210°C and 225°C[15] marking the start of the second section.

The first section, from 170°C to approximately 210°C, consists of at least three steps and results in 1/3 mass loss. As well as the B–H stretches mentioned above, C–H stretches (2790–2970 cm^{-1}) are clearly evident, implying the cyclam ring is already breaking–up at this early stage and explaining the high mass loss. This high mass loss is used to rule out contamination with other organic species as follows: since no volatile Ni species is seen in the MS data, Ni is not responsible for any mass loss; the remaining non–cyclam constituents of Ni(cyclam)(BH$_4$)$_2$ (*i.e.* the two BH$_4$ groups) make up approximately 10% of the total mass; even if all the BH$_4$ mass is lost, it is not credible that the remaining 20%+ mass loss could arise from contaminants not detected in the original sample. Thus, the cyclam ring must disintegrate.

Table ESI_2 Fragments of [HN–(CH$_2$)3–NH]+ that could produce the fragmentation patterns observed in the EGA–MS shown in figure 5

m/z	Fragments of [HN–(CH$_2$)$_3$–NH]$^+$
71,72	[HN–(CH$_2$)$_3$–NH]$^+$ + deprotonation
42,43	[(CH$_2$)$_3$]$^+$, [(CH$_2$)$_2$NH]$^+$ + protonated variants
26,27,30	[CN]$^+$, [HCN]$^+$, [C$_2$H$_2$]$^+$, [C$_2$H$_3$]$^+$, [CH$_3$NH]$^+$
15,16	[CH$_3$]$^+$, [NH]$^+$, [NH$_2$]$^+$
13	[CH]$^+$

The MS data for section 1 (see figure ESI_4 and table ESI_2) show main signals at m/z = 2, 15, 27, 42, 71 whose ratios vary across each of the three steps. In step 1 and step 2, m/z = 27, 42, 71 show significant signals with a profile clearly matching that of mass loss. m/z = 15 rises steadily but slowly across these two steps, m/z = 2 shows very little change. Step 3 of the first section shows significant rises in the signal for m/z = 2, 27, 42, with m/z = 15 remaining steady and m/z = 71 dropping to background levels. These m/z signals fit the fragmentation pattern of THF well, and so could indicate trace contamination (the synthesis was carried out with LiBH$_4$ dissolved in THF). However, the IR spectra (see figure ESI_4) are missing the tell–tale gas–phase THF absorption peaks at 918 and 1080 cm^{-1} which rules this out. The peaks in the MS would also fit fragmentation of the cyclam ring very well (or rather, as we believe, a decomposition product of the cyclam ring). There is no evidence of N–H stretching modes in the EGA–FTIR data, but this does not rule out evolution of amines as the N–H stretches may simply be too weak to detect; nor can the evolution of tertiary amines be ruled out.

The second section of mass loss (above about 215°C) starts with the two endothermic events mentioned above. The second of these events results in the simultaneous detection of particularly strong EGA–MS signals at m/z = 13, 15, 16, 30 and sharp EGA–FTIR signals over the range 3000–3200 cm^{-1}, unique to this point in the TGA/DSC experiment (see figure 5 inset). These FTIR signals do not easily fit either of the two most obvious assignments: the frequency is lower than would typically be expected for

N–H stretches in the gas phase, and alkene C–H stretches are expected to be much broader. The MS signals do not offer much guidance either as their presence could be explained by either of such groups or indeed a molecule containing both. No B–H containing species are detected in the EGA–FTIR of the second section of the TGA/DSC suggesting that all boron has been discharged by this point.

Processes which evolve similar gases continue until about 45% of total mass has been lost, at which point the rate of loss slows considerably but not completely. Considerable decomposition of the cyclam ring must have occurred by this point: assuming two BH_4 groups per molecule have been lost, another 35% must be accounted for – the equivalent of 100 atomic mass units per molecule. Cyclam itself has a formula weight of 200 g mol^{-1}, suggesting that half of the ring has been lost.

The residual fine black powder after cooling from 300°C to room temperature in an Ar flow is amorphous; it will glow red hot on exposure to air and readily set paper alight, probably caused by the presence of nanoparticles of Ni^0.

The greater ease of the cis isomer's thermal decomposition compared to the trans is consistent with the weakened BH bonding in the former isomer, as evidenced by IR spectroscopy. This feature also suggests that the onset of the thermal decomposition is related to a reduction of the Ni(II) center. The cis isomer is better suited for this process due to the presence of spatially proximate coordinated hydrogens of the bidentate BH_4^- group which facilitates evolution of the H_2 molecule. In contrast, the trans isomer's two coordinated hydrogens are separated by the cyclam ring. Evolved gases are essentially identical to those for the trans isomer, with the exception that no EGA–FTIR signals are observed in the CH stretching range (3000–3200 cm^{-1}).

The exothermic decomposition also suggests that both isomers of $Ni(cyclam)(BH_4)_2$ are in fact *metastable* under ambient conditions, their lack of thermodynamic stability arising from both enthalpic and entropic contributions.

S6. Data processing of EGA – MS data

EGA MS ion–currents for each m/z value were normalised such that the minimum ion current for that m/z value over time is set to 1. This means that the values reported in this paper are a multiple of the minimum signal for that m/z value over the whole experiment. The rationale for this approach is that, aside from situations where scavenging occurs, the lowest ion–current will approximate to the background value. Signals that can be seen to be clearly different from background using this method are lost when comparing relative intensity for each scan (i.e., across the whole m/z spectrum at one point in time) due to the huge differences in background ion–current for different m/z. This method allowed us to track changes in signals more easily, but with the effect that isothermal values for different m/z values should not necessarily be considered relative to one another as one would in a typical mass spectrum.

S7. Milling of $Ni(cyclam)(BH_4)_2$ with $NaBH_4$ and particle size effects

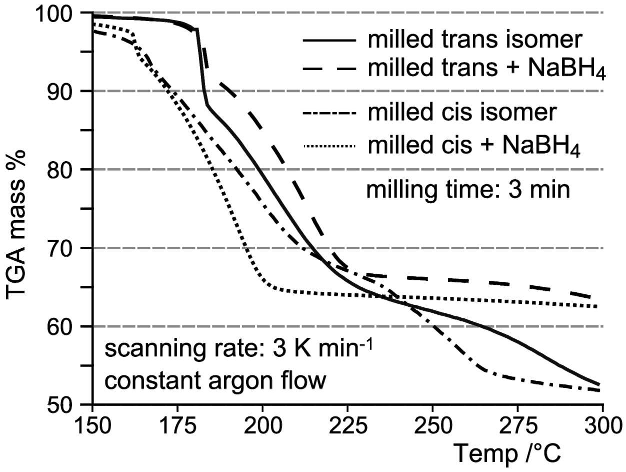

Fig. ESI_5 TGA curves for milled samples of the trans isomers, trans + $NaBH_4$,the cis isomer and cis + $NaBH_4$

Simply milling trans–$Ni(cyclam)(BH_4)_2$ does affect the decomposition profile, with mass loss occurring abruptly around 180–185°C rather than gradually from 160–200°C (see figure ESI_5).

Milling trans–$Ni(cyclam)(BH_4)_2$ with $NaBH_4$ (4.9:1 mole ratio), however, does not alter the profile beyond the effects of milling, with emission of B–H containing species and degradation of the cyclam ligand. However, the total mass loss up to 350°C (further than shown in fig ESI_5) is greater than would be expected if the $NaBH_4$ lay inert (calc. mass loss: 31%, meas.: 41%), suggesting there may be a reaction involving the two compounds. Milling trans–$Ni(cyclam)(BH_4)_2$ with $NaBD_4$ results in exchange of BH_4 ligands preventing use of D_2 detection in EGA–MS to determine at what point such a reaction occurs. Nevertheless, it is clear that this process is not catalytic and so was not investigated further.

Milling cis–$Ni(cyclam)(BH_4)_2$ with $NaBH_4$ (4.4:1 mole ratio) shows a similar decomposition profile as the pure complex, but in this case the mass loss is within the margin of error of what would be expected if the $NaBH_4$ remains unchanged (calc. mass loss: 36%, meas.: 38%).

S8. Results of the DFT calculations

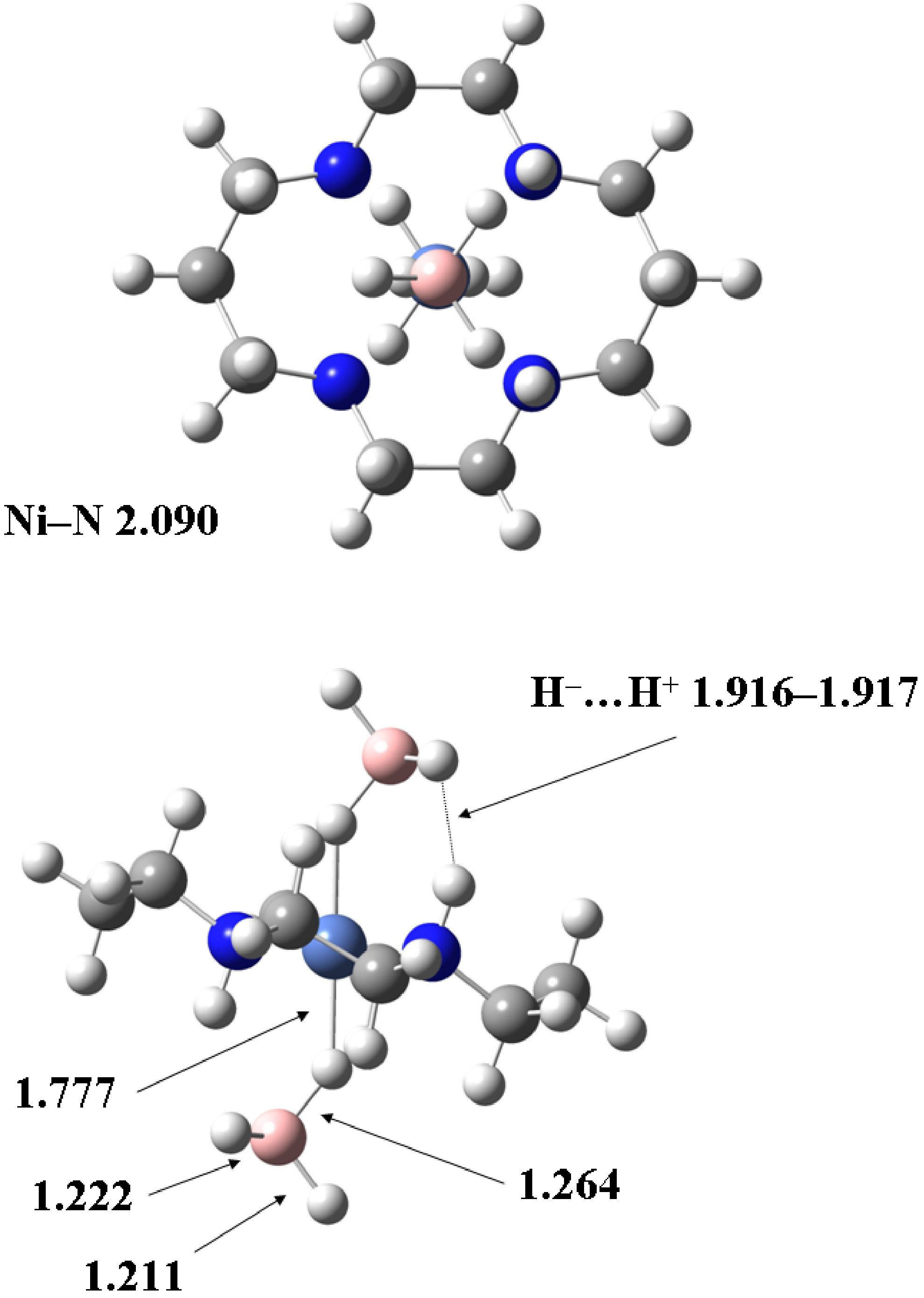

Fig. ESI_6 The DFT–optimized geometry of high–spin trans Ni(cyclam)$(BH_4)_2$ free from crystal lattice distortions (C_{2h}); note the elongation of the bridging BH bond with respect to the remaining ones, by ca. 0.04–0.05 Å; two times larger elongation by 0.08–0.13 Å is seen in the crystal structure possibly as an effect of the intermolecular interactions and crystal packing effects.

Cartesian atomic coordinates for trans-Ni(cyclam)(BH$_4$)$_2$:

Center	Atomic	Atomic	Coordinates (Angstroms)		
Number	Number	Type	X	Y	Z
1	6	0	-1.524024	-3.007236	0.000000
2	1	0	-2.538873	-2.592123	0.000000
3	1	0	-1.642906	-4.095258	0.000000
4	6	0	-0.804723	-2.623570	1.299784
5	1	0	-1.283069	-3.145144	2.140720
6	1	0	0.238025	-2.950177	1.258065
7	7	0	-0.804723	-1.167334	1.535716
8	1	0	-1.767744	-0.823898	1.573559
9	6	0	-0.095689	-0.759079	2.764991
10	1	0	0.878248	-1.255769	2.764902
11	1	0	-0.634288	-1.067957	3.669865
12	6	0	0.095689	0.759079	2.764991
13	1	0	-0.878248	1.255769	2.764902
14	1	0	0.634288	1.067957	3.669865
15	7	0	0.804723	1.167334	1.535716
16	1	0	1.767744	0.823898	1.573559
17	6	0	0.804723	2.623570	1.299784
18	1	0	1.283069	3.145144	2.140720
19	1	0	-0.238025	2.950177	1.258065
20	5	0	2.690754	-1.049463	0.000000
21	6	0	1.524024	3.007236	0.000000
22	1	0	2.538873	2.592123	0.000000
23	1	0	1.642906	4.095258	0.000000
24	6	0	0.804723	2.623570	-1.299784
25	1	0	1.283069	3.145144	-2.140720
26	1	0	-0.238025	2.950177	-1.258065
27	7	0	0.804723	1.167334	-1.535716
28	1	0	1.767744	0.823898	-1.573559
29	6	0	0.095689	0.759079	-2.764991
30	1	0	-0.878248	1.255769	-2.764902
31	1	0	0.634288	1.067957	-3.669865
32	6	0	-0.095689	-0.759079	-2.764991
33	1	0	0.878248	-1.255769	-2.764902
34	1	0	-0.634288	-1.067957	-3.669865
35	7	0	-0.804723	-1.167334	-1.535716
36	1	0	-1.767744	-0.823898	-1.573559
37	6	0	-0.804723	-2.623570	-1.299784
38	1	0	-1.283069	-3.145144	-2.140720
39	1	0	0.238025	-2.950177	-1.258065
40	5	0	-2.690754	1.049463	0.000000
41	28	0	0.000000	0.000000	0.000000
42	1	0	-1.426202	1.061826	0.000000
43	1	0	-3.018327	2.215151	0.000000
44	1	0	-3.059536	0.466854	1.008714
45	1	0	-3.059536	0.466854	-1.008714
46	1	0	3.018327	-2.215151	0.000000
47	1	0	1.426202	-1.061826	0.000000
48	1	0	3.059536	-0.466854	1.008714
49	1	0	3.059536	-0.466854	-1.008714

Mulliken atomic spin densities for trans-Ni(cyclam)(BH$_4$)$_2$ (only values comparable to ±0.01e or larger have been listed):

		1
1	C	-0.010565
4	C	0.012684
17	C	0.012684
20	B	0.125105
21	C	-0.010565
24	C	0.012684
37	C	0.012684
40	B	0.125105
41	Ni	1.903911
42	H	-0.098451
47	H	-0.098451

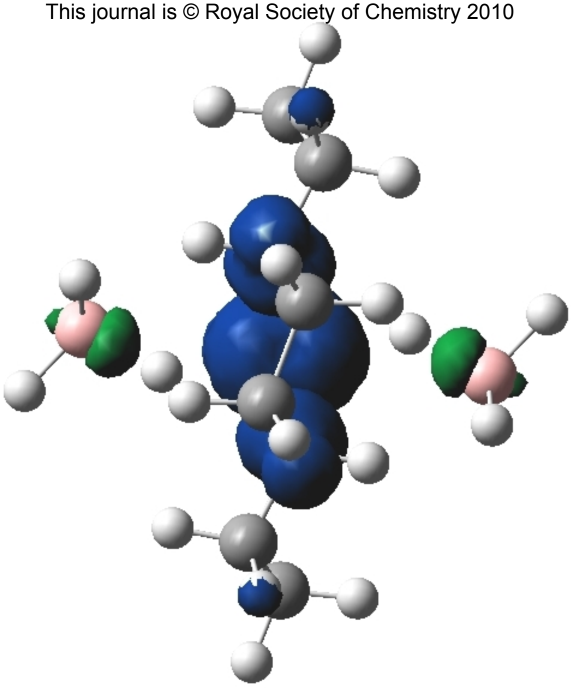

Fig. ESI_7 The DFT–derived spin density for trans Ni(cyclam)$(BH_4)_2$ (C_{2h}) at the ±0.01 e isovalue. Blue and green colours symbolize excess of α and β density, respectively.

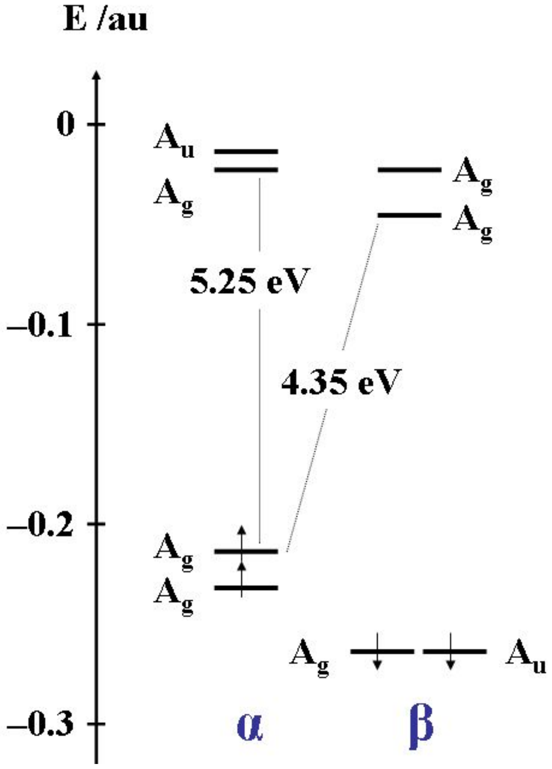

Fig. ESI_8 The DFT–derived MO structure of trans Ni(cyclam)$(BH_4)_2$ (C_{2h}) (α and β orbitals).

The lowest spin- and symmetry-allowed electronic transitions calculated for trans Ni(cyclam)$(BH_4)_2$ using a time-dependent (TD) DFT method. Transitions 1–7 are forbidden. f stands for oscillator strength. Note that Ni(cyclam)$(BH_4)_2$ is not deeply coloured, while its light green might correspond to some weak lower energy absorptions (calculated to range from 1.6414 eV = 755.35 nm) allowed by distortions of molecular structure from C_{2h} while in the crystal lattice.

```
 Excited State   8:   Spin  3-AU     4.8300 eV  256.70 nm  f=0.0068
     80A -> 82A        0.99034

Excited State   9:   Spin  3-BU     4.8597 eV  255.13 nm  f=0.0107
```

```
   80A -> 83A       0.88063
   78B -> 79B      -0.45599

 Excited State  10:    Spin  3-BU     4.8682 eV  254.68 nm  f=0.0317
   80A -> 83A       0.45951
   78B -> 79B       0.87935
```

The computed energy difference (including ZPE) between (optimized) singlet and triplet trans Ni(cyclam)$(BH_4)_2$ is as large as 0.68 eV; the 'vertical' difference must be even larger, which suggests that the NiN_4H_2 complex is far from spin crossover.

Cartesian coordinates for singlet trans Ni(cyclam)$(BH_4)_2$:

Center Number	Atomic Number	Atomic Type	Coordinates (Angstroms) X	Y	Z
1	6	0	0.437222	-3.345035	0.000000
2	1	0	-0.628484	-3.594278	0.000000
3	1	0	0.986257	-4.291111	0.000000
4	6	0	0.799375	-2.581467	1.265028
5	1	0	0.637507	-3.220146	2.141884
6	1	0	1.853964	-2.291582	1.248689
7	7	0	0.000000	-1.344538	1.422955
8	1	0	-1.005330	-1.597175	1.422409
9	6	0	0.336492	-0.676875	2.701834
10	1	0	1.422782	-0.563039	2.743619
11	1	0	0.016090	-1.281429	3.557100
12	6	0	-0.336492	0.676875	2.701834
13	1	0	-1.422782	0.563039	2.743619
14	1	0	-0.016090	1.281429	3.557100
15	7	0	0.000000	1.344538	1.422955
16	1	0	1.005330	1.597175	1.422409
17	6	0	-0.799375	2.581467	1.265028
18	1	0	-0.637507	3.220146	2.141884
19	1	0	-1.853964	2.291582	1.248689
20	5	0	2.972965	1.249652	0.000000
21	6	0	-0.437222	3.345035	0.000000
22	1	0	0.628484	3.594278	0.000000
23	1	0	-0.986257	4.291111	0.000000
24	6	0	-0.799375	2.581467	-1.265028
25	1	0	-0.637507	3.220146	-2.141884
26	1	0	-1.853964	2.291582	-1.248689
27	7	0	0.000000	1.344538	-1.422955
28	1	0	1.005330	1.597175	-1.422409
29	6	0	-0.336492	0.676875	-2.701834
30	1	0	-1.422782	0.563039	-2.743619
31	1	0	-0.016090	1.281429	-3.557100
32	6	0	0.336492	-0.676875	-2.701834
33	1	0	1.422782	-0.563039	-2.743619
34	1	0	0.016090	-1.281429	-3.557100
35	7	0	0.000000	-1.344538	-1.422955
36	1	0	-1.005330	-1.597175	-1.422409
37	6	0	0.799375	-2.581467	-1.265028
38	1	0	0.637507	-3.220146	-2.141884
39	1	0	1.853964	-2.291582	-1.248689
40	5	0	-2.972965	-1.249652	0.000000
41	28	0	0.000000	0.000000	0.000000
42	1	0	-2.427076	-0.139645	0.000000
43	1	0	-4.177660	-1.134214	0.000000
44	1	0	-2.614164	-1.878608	1.005063
45	1	0	-2.614164	-1.878608	-1.005063
46	1	0	4.177660	1.134214	0.000000
47	1	0	2.427076	0.139645	0.000000
48	1	0	2.614164	1.878608	1.005063
49	1	0	2.614164	1.878608	-1.005063

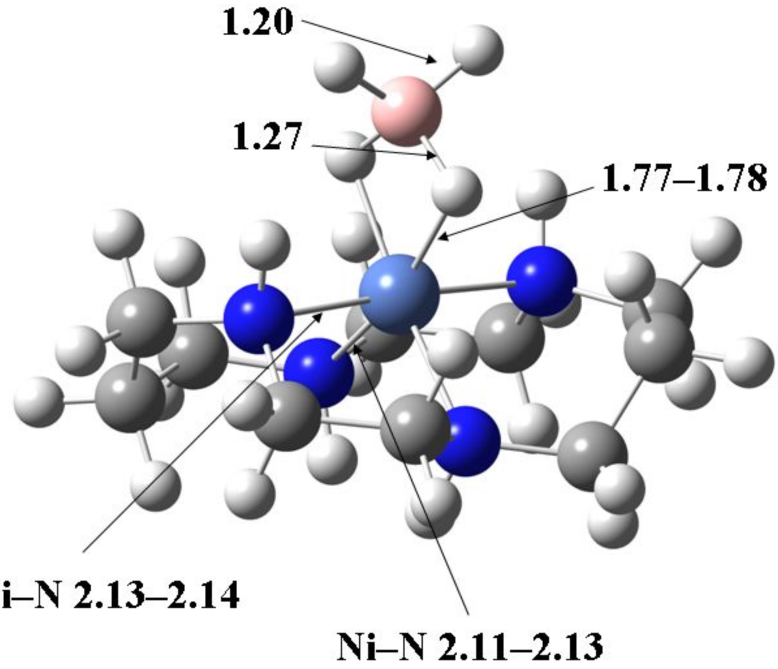

Fig. ESI_9 The DFT–derived molecular structure of cis Ni(cyclam)(BH$_4$)$^+$ (C$_1$). Note the elongation of the bridging BH bonds by 0.07 Å with respect to the terminal ones.

Mulliken atomic spin densities for cis-Ni(cyclam)(BH$_4$)$_2$ (only values comparable to ±0.01e or larger have been listed):

1	Ni	1.815461
8	C	-0.011793
11	C	0.016450
12	B	0.115913
16	C	-0.011970
41	H	0.027699

Cartesian atomic coordinates for triplet cis-Ni(cyclam)(BH$_4$)$^+$:

Center Number	Atomic Number	Atomic Type	Coordinates (Angstroms)		
			X	Y	Z
1	28	0	0.001215	0.000761	-0.003543
2	7	0	0.002241	0.000833	2.136032
3	7	0	2.119088	-0.003575	0.261241
4	7	0	0.119011	-0.055991	-2.134135
5	7	0	-0.358725	-2.068029	-0.192429
6	6	0	1.407376	0.064445	2.602425
7	6	0	2.277698	0.731967	1.542662
8	6	0	2.944875	0.546574	-0.860682
9	6	0	1.248034	0.664871	-2.802353
10	6	0	-0.684804	-2.434072	2.271536
11	6	0	-0.826963	-1.016417	2.833634
12	5	0	-1.460406	1.640700	-0.043744
13	6	0	-0.919896	-2.214438	-1.559914
14	6	0	-0.036426	-1.468940	-2.554453
15	6	0	2.162014	1.425848	-1.837777
16	6	0	-1.242529	-2.635189	0.859872
17	1	0	2.440279	-0.952527	0.438239
18	1	0	-0.738618	0.445550	-2.356722
19	1	0	0.519254	-2.584965	-0.164424
20	1	0	-0.434834	0.905305	2.304772
21	1	0	3.324080	0.749060	1.867341
22	1	0	1.958947	1.764216	1.379987
23	1	0	1.762264	-0.955943	2.776238
24	1	0	1.493511	0.598655	3.554266
25	1	0	-0.588020	-1.023178	3.903874
26	1	0	-1.867599	-0.696786	2.741440
27	1	0	-1.232155	-3.103216	2.941756
28	1	0	0.358020	-2.771993	2.316337

29	1	0	-1.399943	-3.703961	0.672894
30	1	0	-2.213705	-2.141844	0.767650
31	1	0	-1.013959	-3.267111	-1.848927
32	1	0	-1.923278	-1.781687	-1.547786
33	1	0	0.958283	-1.924400	-2.578994
34	1	0	-0.454557	-1.556687	-3.563019
35	1	0	1.841727	-0.063886	-3.361577
36	1	0	0.840963	1.366463	-3.534005
37	1	0	2.891211	1.970205	-2.446823
38	1	0	1.592538	2.184178	-1.294945
39	1	0	3.382859	-0.299536	-1.398335
40	1	0	3.780174	1.115916	-0.441459
41	1	0	-1.723581	0.394722	-0.063393
42	1	0	-0.198335	1.765400	0.021432
43	1	0	-1.932447	2.101857	0.959899
44	1	0	-1.832900	2.116254	-1.081673

Cartesian coordinates for singlet cis Ni(cyclam)$(BH_4)_2$:

Center Number	Atomic Number	Atomic Type	Coordinates (Angstroms) X	Y	Z
1	28	0	0.042429	-0.038640	0.824871
2	7	0	-2.217978	-1.183979	0.202264
3	7	0	0.626174	-1.346381	-0.557964
4	7	0	2.217357	1.152604	-0.124460
5	7	0	-0.635580	1.419087	-0.394829
6	6	0	-1.788053	-1.898238	-0.997515
7	6	0	-0.376291	-2.431083	-0.804695
8	6	0	1.973981	-1.993569	-0.352998
9	6	0	3.209081	0.253485	-0.715996
10	6	0	-3.121998	0.956751	-0.694090
11	6	0	-3.413234	-0.347086	0.051979
12	5	0	0.338415	-0.032197	2.833791
13	6	0	0.285048	2.600056	-0.388172
14	6	0	1.665003	2.234137	-0.923256
15	6	0	3.145846	-1.082507	0.028513
16	6	0	-2.043212	1.850884	-0.081047
17	1	0	0.704301	-0.813283	-1.423173
18	1	0	2.538908	1.488609	0.777271
19	1	0	-0.656376	1.083238	-1.358189
20	1	0	-2.354492	-1.843929	0.961020
21	1	0	-0.071282	-3.022642	-1.674379
22	1	0	-0.349530	-3.089828	0.066589
23	1	0	-1.813143	-1.211928	-1.850307
24	1	0	-2.445982	-2.737735	-1.265888
25	1	0	-4.231124	-0.875926	-0.459763
26	1	0	-3.770237	-0.108025	1.056964
27	1	0	-4.050377	1.534680	-0.723266
28	1	0	-2.879686	0.760719	-1.746201
29	1	0	-2.173805	2.865079	-0.471217
30	1	0	-2.145579	1.902944	1.004174
31	1	0	-0.147854	3.404656	-0.992136
32	1	0	0.353383	2.955689	0.642500
33	1	0	1.573826	1.887571	-1.959632
34	1	0	2.285648	3.140559	-0.959436
35	1	0	2.970206	0.118747	-1.777598
36	1	0	4.229492	0.656961	-0.683759
37	1	0	4.057785	-1.657345	-0.159209
38	1	0	3.126913	-0.877395	1.102668
39	1	0	2.213501	-2.523481	-1.282383
40	1	0	1.841519	-2.749430	0.422910
41	1	0	-0.322464	0.838581	2.070511
42	1	0	0.483383	-1.026187	1.947235
43	1	0	-0.390226	-0.412787	3.693637
44	1	0	1.396364	0.408494	3.164309

The computed energy difference (without ZPE) between (optimized) singlet and triplet cis Ni(cyclam)$(BH_4)_2$ is as large as 1.63 eV; the 'vertical' difference must be even larger, which again suggests that the NiN_4H_2 complex is far from spin crossover.